AIMS Materials Science, 9(5): 684–701.
DOI: 10.3934/matersci.2022042
Received: 04 July 2022
revised: 07 August 2022
Accepted: 12 August 2022,
Published: 01 September 2022

http://www.aimspress.com/journal/Materials

Research article

On Λ-Fractional peridynamic mechanics

K.A. Lazopoulos[1,*], E. Sideridis[2] and A.K. Lazopoulos[3]

1 Independent researcher
2 SEMFE, National Technical University of Athens, Greece
3 Mathematical Sciences Department, Hellenic Army Academy, Vari, Greece

* **Correspondence:** Email: kolazop@mail.ntua.gr.

Supplementary

S1. The homogenized composite materials theory, (Theory and experimental evidence)

Proceeding to the formulation of the composite particulate materials, a spherical particulate, and a spherical composite material are considered, see Figure 12.

Following Spathis et al [24] the homogenized Young's modulus E_c and Poisson's ratio ν_c depend upon the various characteristics of the materials. In fact,

$$E_c = E_c\,(E_f, \nu_f, E_m, \nu_m, \lambda, U_f, U_m) \tag{S1}$$

$$\nu_c = \nu_c\,(E_f, \nu_f, E_m, \nu_m, U_f, U_m) \tag{S2}$$

$$U_f = r_f^3 / r_m^3 \tag{S3}$$

$$U_m = (r_m^3 - r_f^3) / r_m^3 \tag{S4}$$

In the above relations, E_f, ν_f, U_f, r_f and E_m, ν_m, U_m, r_m are the Elastic modulus, Poisson ratio, volume fraction, and radius of the fillers and the matrix respectively, whereas λ denotes the relationship between the applied pressure P_1 to the composite with the common stress P_0 at the inclusion-matrix interface, as $\lambda = P_0 / P_1$. By modifying the model used in Ref. [24] so that be applied for the two-phase composite, the Elastic modulus, E_c, can be obtained. Concerning Poisson's ratio of the composite, the difference in the values of the Poisson ratios of the inclusions and the matrix is very small. Thus, the

Poisson ratio of the composite, ν_c, may be evaluated with accuracy by the law of mixtures (or the inverse law of mixtures) as follows:

$$\nu_c = \nu_f U_f + \nu_m U_m \tag{S5}$$

$$\frac{1}{\nu_c} = \frac{U_f}{\nu_f} + \frac{U_m}{\nu_m} \tag{S6}$$

$$\frac{2(1-2\nu_c)}{E_c} = 2\lambda^2(1-2\nu_f)\frac{U_f}{E_f} + \frac{U_f(1-\lambda)^2(1+\nu_m) + 2(\lambda U_f - 1)^2(1-2\nu_m)}{(1-U_f)E_m} \tag{S7}$$

where λ is obtained by Eq S8:

$$\lambda = \frac{3(1-\nu m)Ef}{2Uf(1-2\nu m)+1+\nu m)]Ef+2(1-2\nu f)(1-Uf)Em} \tag{S8}$$

Similarly, from the modified model of Ref. [24], the radial stresses and displacements are obtained as Eqs S9–S12:

$$\sigma_{r,f} = -P_0 = -\lambda P_1 \tag{S9}$$

$$\sigma_{r,m} = \frac{r_f^3(\lambda-1)P_1}{1-U_f}\frac{1}{r^3} + \frac{(\lambda U_f - 1)P_1}{E_m(1-U_f)}\, r \tag{S10}$$

$$u_{r,f} = -\frac{\lambda P_1(1-2\nu_f)r}{E_f} \tag{S11}$$

$$u_{r,m} = \frac{(r_f^3(\lambda-1)+\nu_m)P_1}{2(1-U_f)E_m}\frac{1}{r^2} + \frac{(1-2\nu_m)(\lambda U_f - 1)P_1}{E_m(1-U_f)}r \tag{S12}$$

S2. Material and experimental work

The properties of the constituent materials are presented in Table S1. The matrix material that was used was diglycidyl ether of bisphenol-A resin, with the commercial designation Epikote 828 by Shell Co. as prepolymer, with an epoxy equivalent 185–192, molecular weight between 370 and 384 and viscosity of 15000 cP at 25 °C. As a curing agent, 8% triethylenetetramine hardener per weight of the epoxy resin was employed. Next, the mixture after being stirred thoroughly was put in a vacuum chamber for about 15 min for degassing. Then, it was cast into a rectangular Plexiglas mould suitable and coated with silicon oil to prevent adhesion of the mixture to it. The latter was then sealed so that it was possible to rotate it to prevent the aluminum powder from settling and to obtain as uniform a final product as possible. As the pot life of the matrix material is of the order of 20 °C at ambient

temperature, which was slightly decreased by the presence of the particles, it only took 20–25 min for the mixture to gel, after which no more rotating was necessary. The moulding was removed 24 h later and the casting was subjected to thermal processing, consisting of a temperature rise at 5 ℃/h maintained constant at 100 ℃ and finally dropped to ambient at 1 ℃/h. In this manner, complete polymerization of the matrix material was obtained and consequently, the properties of the final product did not exhibit any storage dependence. Five filler volume fractions (0.05; 0.10; 0.15; 0.20; 0.30) were used. The test pieces were machined from each casting. The composite density was measured for each volume fraction. The following values concerning the aluminum particles were provided by the manufacturers.

The aluminium powder of a single particle size containing 0.2% Al_2O_3 in the form of spheroidal had the following size (diameter) distribution: 0.16 mm, traces; +0.125 mm, 0.5%, 0.04 mm, 10–12% under 0.04 mm 80–90% were added. Thus, the radius r_f is taken as $r_f = 20\ \mu = 0.020$ mm.

Table S1. Properties of constituent materials.

Property	Aluminum	Epoxy resin
Elastic Modulus [E] (N/m^2)	70×10^9	3.5×10^9
Bulk modulus [K] (N/m^2)	73×10^9	4.2×10^9
Poisson ratio [v]	0.34	0.36
Density [ρ] (kg/m^3)	2700	1190
Thermal expansion coefficient [α] (C^{-1})	22.4×10^{-6}	60.26×10^{-6}

To measure the elastic modulus of the particulate composite, tensile experiments were carried out with an Instron-type testing machine at room temperature. Four specimens of each material were tested at a rate of extension of 1 mm/min. The specimens used were of dogbone type with dimensions at the measuring region $(50 \times 20 \times 9) \times 10^{-3}$ m and of a total length 150×10^{-3} m. To obtain the strains for each material, strain gauges (KYOWA type, gauges factor k = 1.99) were located on each specimen to measure the strains. Each value on the diagram is the mean value of the obtained results.

S3. Results

Figure 12 illustrates the variation of composite density vs the filler volume fraction as obtained from the experiments. As expected, the density increases with the addition of aluminum particles in the epoxy resin. In Figure 13, the variation of composite Poisson ratio vs filler volume fraction calculated from Eqs S6,S7. It can be observed that, as expected, the Poisson ratio decreases with the addition of particles and that there is no significant difference in the values derived from the two laws of mixtures.

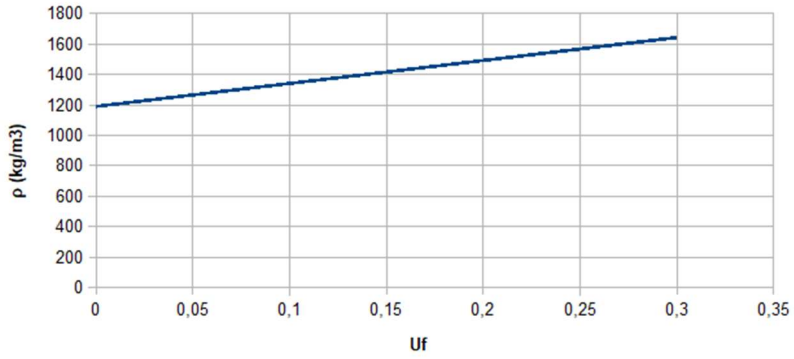

Figure S1. Density of the composite material vs the filler volume fraction.

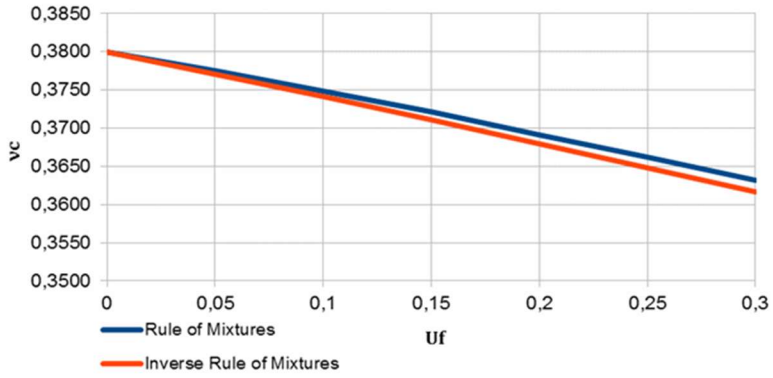

Figure S2 Poisson's radio of the composite material vs the filler volume fraction.

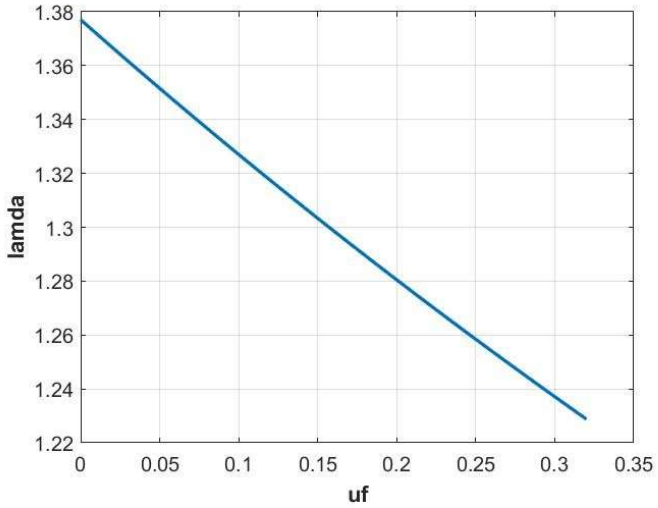

Figure S3 Variation of λ (lamda) vs filler volume fraction.

The variation of the coefficient λ (lamda), mentioned previously, as denoting the relationship between the applied stress P_1 applied to the composite and the stress P_0 in the filler-matrix interface, vs volume fraction Uf calculated from Eq S8 is illustrated in Figure S3. It can be observed that λ decreases as U_f increases. It means that the addition of particles in the matrix decreases the stress at the interface. This interaction of the aluminum inclusions surface with epoxy resin is usually more complicated than a simple mechanical effect. The presence of the inclusions restricts the segmental and molecular mobility of the polymer, as absorption interaction in epoxy resin surface layers into aluminum particles occurs.

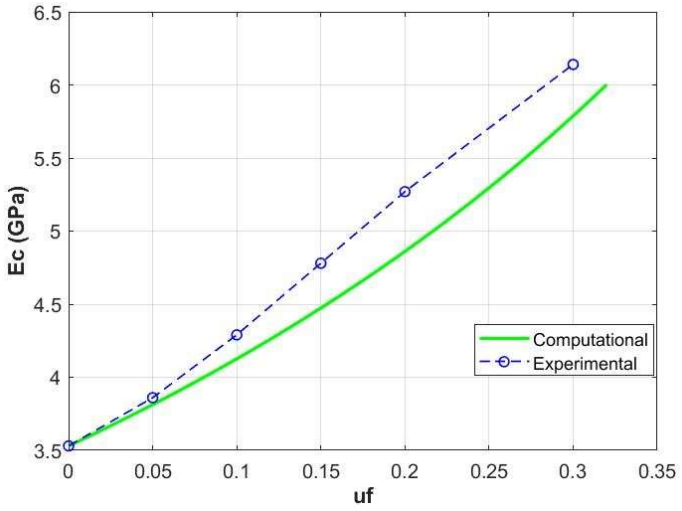

Figure S4 Variation of composite modulus vs filler volume fraction.

The variation of the composite modulus Ec vs volume fraction U_f was plotted in Figure S4. Theoretical values obtained from Eq S7 were compared to experimental results. In both cases, the addition of aluminum particles augments the stiffness of the polymeric matrix. However, there is a discrepancy between theory and experiment when the volume fraction increases. Although it is assumed that the volume fraction of the inclusions is small, so that the interaction among them may be neglected, it can be said that in reality such an interaction normally exists. Therefore, it can be concluded that the theoretical values obtained from Eq S8 for the elastic modulus are valid for low volume fractions. For higher volume fractions a theory, which will consider the adhesion efficiency and the interaction between epoxy and aluminum particles by taking into account their distribution in the matrix or their arrangement (see Figure S8), should be used. Finally, as was previously mentioned in the material description, all the inclusions do not have the same size (radius), which was taken as 20 μ, i.e., r_f = 0.020 mm. This fact does not appear in the theoretical formula (Eq S8) but may affect experimental results.

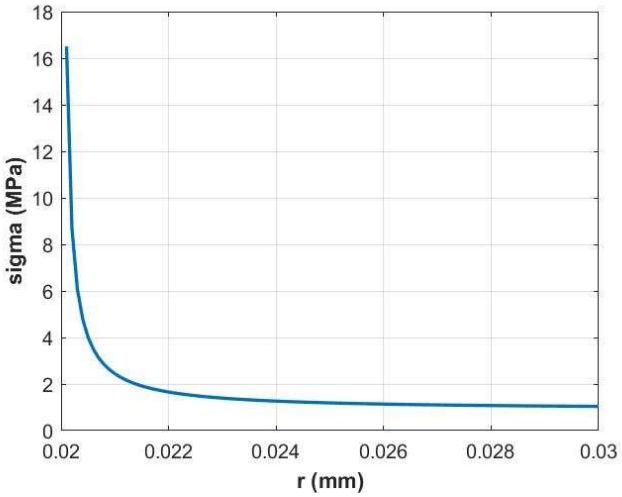

Figure S5. Variation of radial stress vs radius.

Now, let us calculate the radial stress and the radial displacement in the composite for a certain volume fraction. By choosing the largest value used in the experiments, namely for $U_f = 0.030$, with filler inclusion $r_f = 20$ μ., we have $r_m = 29.756$ μ. The variation of the radial stress σ_r (sigma) vs radius is illustrated in Figures S5,S6, taking into consideration Eqs S9,S10, Eq S8 and that the radius of the aluminum particles is 20 μ. (0.020 mm), it can be observed that there is an abrupt decrease in stress, up to 0.021 mm. Later, a smoother decrease occurs up to 0.024 mm and then tends asymptotically to the horizontal axis.

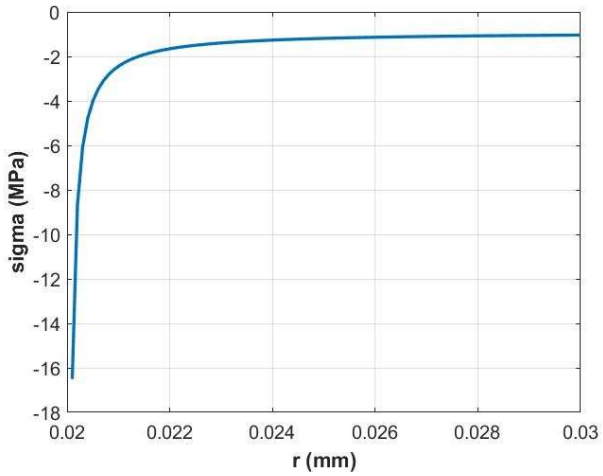

Figure S6. Variation of radial stress vs radius.

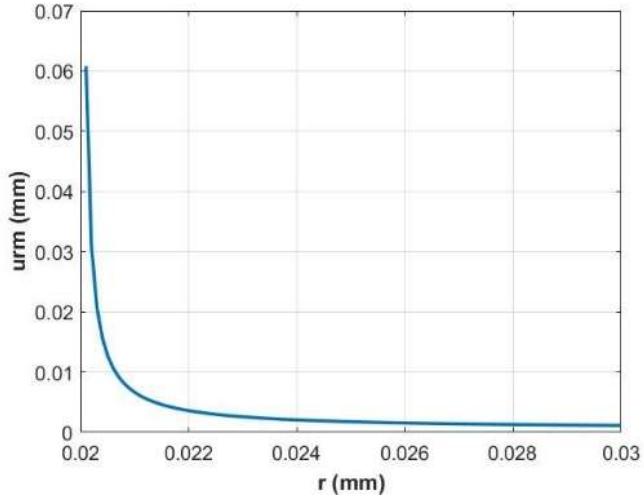

Figure S7. Variation of displacement vs radius.

In Figure S7 the variation of the radial displacement u_r is plotted vs radius, by taking into consideration Eqs S9,S10. A similar behavior to that of stress can be observed. An abrupt decrease after the filler radius 0.020 mm, then a small decrease up to 0.024 mm, and finally, a slight decrease where the curve tends as in the previous case, almost asymptotically to the horizontal axis.